Extreme winds in the Western North Pacific

Ott, Søren

Publication date:
2006

Document Version
Publisher's PDF, also known as Version of record

RISØ

Risø-R-1544(EN)

Extreme Winds in the Western North Pacific

Søren Ott

Risø National Laboratory
Roskilde
Denmark
November 2006

Risø-R Report

Author: Søren Ott
Title: Extreme Winds in the Western North Pacific
Department: Wind Energy Department

Risø-R-1544(EN)
November 2006

Abstract (max. 2000 char.):
A statistical model for extreme winds in the western North Pacific is developed, the region on the Planet where tropical cyclones are most common. The model is based on best track data derived mostly from satellite images of tropical cyclones. The methods used to estimate surface wind speeds from satellite images is discussed with emphasis on the empirical basis, which, unfortunately, is not very strong. This is stressed by the fact that Japanese and US agencies arrive at markedly different estimates. On the other hand, best track data records cover a long period of time and if not perfect they are at least coherent over time in their imperfections. Applying the the Holland model to the best track data, wind profiles can be assigned along the tracks. From this annual wind speed maxima at any particular point in the region can be derived. The annual maxima, in turn, are fitted to a Gumbel distribution using a generalization Abild's method that allows for data wind collected from multiple positions. The choice of this method is justified by a Monte Carlo simulation comparing it to two other methods. The principle output is a map showing fifty year winds in the region. The method is tested against observed winds from Philippine synoptic stations and fair agreement is found for observed and predicted 48–year maxima.
However, the almost bias–free performance of the model could be fortuitous, since precise definitions of 'windspeed' in terms averaging time, height above ground and assumed surface roughness are not available, neither for best tracks nor for the synoptic data.
The work has been carried out under Danish Research Agency grant 2104-04-0005 "Offshore wind power" and it also covers the findings and analysis carried out in connection with task 1.6 of the project "Feasibility Assessment and Capacity Building for Wind Energy Development in Cambodia, The Philippines and Vietnam" during 2005-06 under contract 125-2004 with EU-ASEAN Centre of Energy.

ISSN 0106-2840
ISBN 87-550-3500-0

Contract no.:

Group's own reg. no.:
(Føniks PSP-element)

Sponsorship:

Cover :

Pages: 36
Tables: 3
References: 26

Risø National Laboratory
Information Service Department
P.O.Box 49
DK-4000 Roskilde
Denmark
Telephone +45 46774004
bibl@risoe.dk
Fax +45 46774013
www.risoe.dk

Abstract A statistical model for extreme winds in the western North Pacific is developed, the region on the Planet where tropical cyclones are most common. The model is based on best track data derived mostly from satellite images of tropical cyclones. The methods used to estimate surface wind speeds from satellite images is discussed with emphasis on the empirical basis, which, unfortunately, is not very strong. This is stressed by the fact that Japanese and US agencies arrive at markedly different estimates. On the other hand, best track data records cover a long period of time and if not perfect they are at least coherent over time in their imperfections. Applying the the Holland model to the best track data, wind profiles can be assigned along the tracks. From this annual wind speed maxima at any particular point in the region can be derived. The annual maxima, in turn, are fitted to a Gumbel distribution using a generalization Abild's method that allows for data wind collected from multiple positions. The choice of this method is justified by a Monte Carlo simulation comparing it to two other methods. The principle output is a map showing fifty year winds in the region. The method is tested against observed winds from Philippine synoptic stations and fair agreement is found for observed and predicted 48–year maxima. However, the almost bias–free performance of the model could be fortuitous, since precise definitions of 'windspeed' in terms averaging time, height above ground and assumed surface roughness are not available, neither for best tracks nor for the synoptic data.

The work has been carried out under Danish Research Agency grant 2104-04-0005 "Offshore wind power" and it also covers the findings and analysis carried out in connection with task 1.6 of the project "Feasibility Assessment and Capacity Building for Wind Energy Development in Cambodia, The Philippines and Vietnam" during 2005-06 under contract 125-2004 with EU-ASEAN Centre of Energy.

Approved by: Lars Landberg

Checked by: Jakob Mann, Niels Jacob Tarp-Johansen

.

Contents

1 Introduction *5*

2 Typhoon data *7*
2.1 The Dvorak method *7*
2.2 TC intensity *8*
2.3 Comparison between JMA and JTWC best track data for 2000–2003 *12*

3 The Holland model *15*

4 Wind turbine loads during an eyewall passage *18*

5 Extreme winds *21*
5.1 The Gumbel distribution *22*
5.2 Estimation of U_{50} *23*
5.3 Comparison of U_{50} estimates *25*

6 Extreme wind atlas for the NW Pacific *27*

7 Validation *29*
7.1 Data from the Province of Batanes *29*
7.2 Comparison with Philippine Extreme wind data *31*

8 Conclusions *34*

1 Introduction

The western North Pacific wind climate is dominated by tropical cyclones, or typhoons as they are called in this part of the world. Tropical cyclones are the most devastating types of storms that exist on the planet, each year causing tremendous damage in terms of loss of lives and property. The purpose here is to estimate the implications for wind turbine design in the western North Pacific area, in particular as quantified by the fifty year wind.

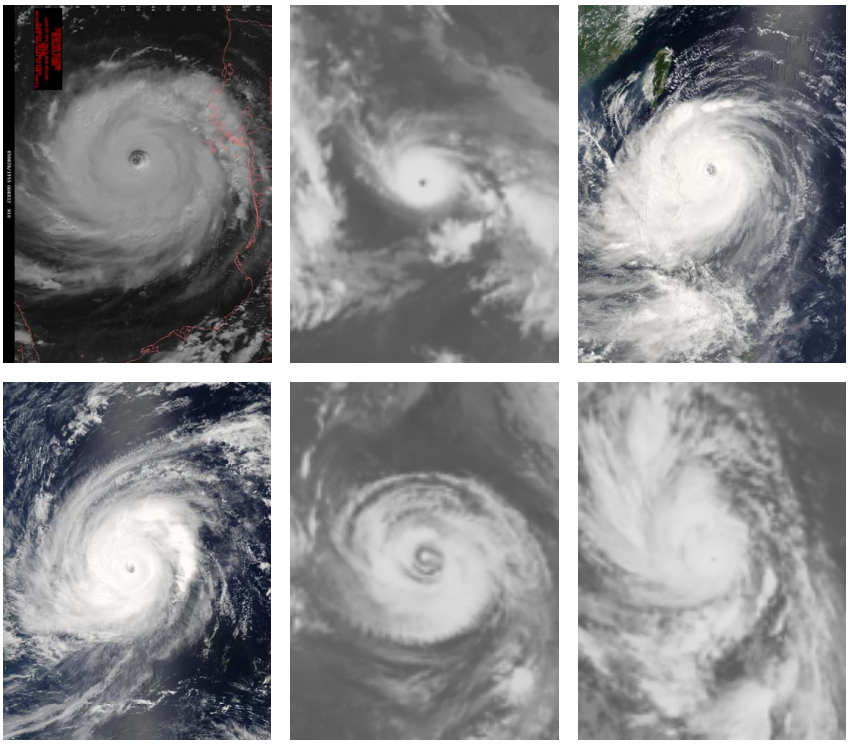

Figure 1. Visible light images of fully developed tropical cyclones.

Cyclones are circulating, low pressure wind systems. Extra-tropical cyclones (outside the tropics) are primarily formed at the interface between two air masses of different temperature, and the temperature difference between them is their main source of energy. The border between the two air masses are the characteristic cold and warm fronts that curl up around the centre. A tropical cyclones (TC) has a warm centre surrounded by relatively colder air and there are no fronts. The energizing mechanism in TCs is the condensation of water vapour supplied by sufficiently warm sea surface. Rising, humid air cause the formation of intense, local thunderstorms which tend to concentrate in spiral shaped rainbands. The central region is covered by a dense overcast, but just at the centre there usually is a circular spot, the 'eye', which is free of clouds. Inside the eye wind speeds are moderate and there can even exist a completely dead calm. This is in contrast to the edge of the eye, the eyewall, where maximum wind speeds are found. Figure 1 shows a few satellite pictures of typical, fully developed tropical cyclones. The eye, the rainbands and the overall circular structure is evident. Even if the individual thunderclouds inside the cyclone are highly irregular, turbulent and random, the overall, large scale, features of the flow appear regular and deterministic, especially near of the core region. This is revealed in greater detail by direct measurements, made e.g. by reconnaissance aircraft that

are able 'scan' the wind and pressure fields. The general pattern is a circulatory motion orbiting the eye resulting from a balance between the centripetal acceleration and a radial pressure gradient. The velocity generally decreases with height because the pressure gradient decreases. Near the surface the friction takes over causing the opposite trend so that the velocity has a maximum found typically at an elevation of about 500m. Below the velocity maximum friction makes the wind turn towards the centre, but near the eye-wall it is caught by a vertically spiralling jet extending 5-10 km up into the troposphere. At the top the jet 'spills over' and splits into an outgoing jet and a jet going back into the eye. The air inside the eye is therefor generally subsiding (decending) and flowing out towards the eyewall along the surface. This explains why there are no clouds in the eye.

The mechanisms that control tropical cyclone genesis are not fully understood, so there is no explanation of why typhoons are particularly frequent in the western North Pacific. It can be shown that tropical cyclones cannot form unless the sea temperature exceeds 26°C. In case of landfall the supply of water vapour is cut and the cyclone deteriorates rapidly, but it can still endanger a zone along the coastline several hundreds of kilometers wide. A warm sea is a necessary condition for tropical cyclone genesis, but it appears not to be the only condition. In fact there are major parts of the tropics, with plenty of warm sea, where tropical cyclones virtually never occur. These areas include the Eastern South Pacific, the South Atlantic (although a TC hit Brazil in March 2004) and a ten degree wide strip around the Equator where the Coriolis parameter is too small for TCs to form .

2 Typhoon data

Tropical cyclones are monitored closely by meteorologists both at national and international levels. Regional warning centers are organized by the World Meteorological Organization (WMO) in the framework of the World Weather Watch (WWW) Programme. Analyses and forecasts of tropical cyclones in the western North Pacific are provided by the RSMC Tokyo-Typhoon Center, which is operated by the Japanese Meteorological Agency (JMA). Independent forecasts for the region are made by the US navy at the Joint Typhoon Warning Center (JTWC) on Hawaii.

Historic typhoon data are available from these sources in the form of so-called 'best tracks'. These are constructed on the basis of all available information, 'hindcasting' rather than forecasting. The amount of details given in track records vary, but as a minimum they contain the center position and the central pressure (at sea level) at 6 hours intervals. The JMA track records cover all tropical cyclones north of the equator in the region between the 100E and 180E meridians (the western North Pacific and the South China Sea) for the period 1951-2004. From 1977 onwards the 'maximum sustained wind', representing the maximum ten minute average wind speed measured ten meter above surface, is also given as well as the radii to 50 knot and 30 knot wind speeds (also ten minutes averages at ten meter). The JTWC tracks contain central pressures and positions for the period 1945-2003. For 2001-2003 the following data are also included: ambient pressure (at the last closed isobar), radius to the last closed isobar, maximum sustained wind, radius of maximum wind and radius of 34 knot surface wind. We note that JTWC, and other US institutions, deviate from the WMO standard and define the maximum sustained wind speeds as a one minute average.

Positions are given to the nearest tenths of a degree, wind speeds are usually rounded to the nearest five knots (i.e. 35,40,55 knots) and distances to the nearest 5 nautical miles. This should not be taken as an indication of the degree of uncertainty of the numbers.

The amount and quality of the information on which the best tracks are estimated is varying. There are generally few conventional surface observations to rely on since met stations, platforms and buoys are relatively scarce in the oceanic region. Velocities at ten meter elevation are therefore inferred from other data. These include satellite pictures, reconnaissance aircraft, radar and radiosonde observations. Of these the reconnaissance aircraft data are the most detailed, but they are not always available in the Pacific and were not available in the past.

Most of the JTWC tracks are based on satellite image interpretation by the Dvorak method (see below), since other direct observations seldom are available. The central pressure and the maximum sustained wind are in fact rarely measured. JMA uses different methods which are probably also based almost entirely on satellite images.

2.1 The Dvorak method

This method is an attempt to estimate the various parameters describing a tropical cyclone from satellite images. The basic observation is that the images show progressively more distinct and circular features as the cyclone intensifies. The technique was developed by Dvorak (1975) who defined a set of rules to determine a so called T-number characterizing the stage of development. The T-numbers are assigned mainly from individual images although an assessment of the development on the basis of earlier images is also involved. No attempt is made to make velocimetry from consecutive images, probably because they are too far apart in time, so the method totally relies on the recognition of shapes and patterns and to some degree also on the absolute sizes of these. In later versions visible images are supplemented by EIR (Enhanced Infra Red) images which do not depend on daylight and also in some cases can yield quantitative information on the temperatures at the cloud-tops as well as in the eye. The T-numbers range on a scale from T1 to T8 and

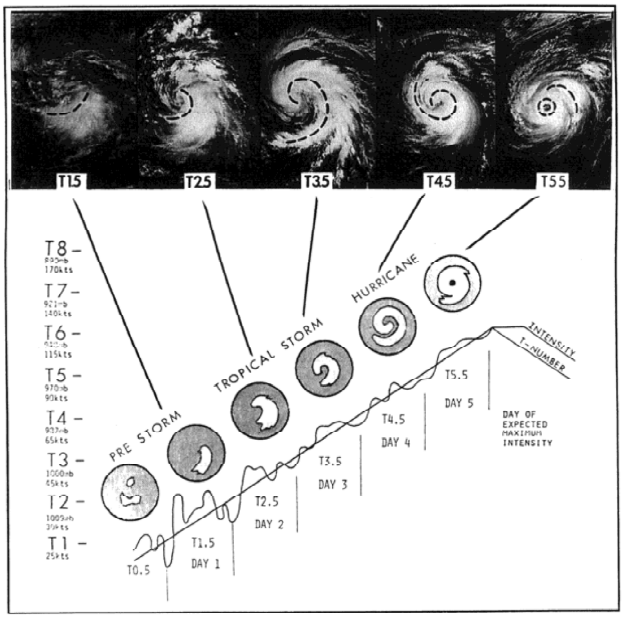

Figure 2. Illustration of the Dvorak method.

are given in steps of one half. Although an effort has been made to formulate the rules so as to eliminate subjectiveness, different evaluators do not always end up with the same T-number. However, experience shows that variations are within ± 1. Finally, Dvorak offers a table assigning a central pressure and a maximum sustained wind to each T-number (without explaining how it came about). This implicitly postulates a relation between P_c and V_{max}, which turns out to be identical to the one given by Atkinson and Holliday (1977), and which will be commented on below. The validation of the early version of the method consisted in a comparison with estimates of V_{max} made by JTWC for the year 1972, where the mean error of V_{max} were found to be 8 knots (plus or minus?) with a standard deviation of 12 knots. Later validations were reviewed by Harper (2002) who discussed the empirical foundation of the method. From this it appears that the method is objective in the sense that the T–number assignment is reproducible, but that the last step of the process, the assignment of a maximum sustained wind to the T-number, has essentially not been validated since 1975.

2.2 TC intensity

The maximum sustained wind $V_{\max}$ is the proper intensity measure in many applications, but it is not an easy concept to work with. It is supposed to denote the ten minutes average wind speed at ten meter found anywhere in the system at any given time. It therefore requires detailed knowledge of the whole wind field, which in real life is not attainable. Reconnaissance aircraft measurements of wind speed may give the best indication, but since they are taken at elevated positions (typically at 700mb), they are only surrogates for the surface measurements. Alternatively the maximum sustained wind can be interpreted as the maximum (time averaged) wind measured by a fixed anemometer during passage of the eye. However, surface measurements are scarce on deep seas and anemometers tend to be damaged in very strong winds. Strong winds may also be out of the calibrated range. In most cases there are therefore very few, if any, surface wind speed measurements to rely on.

The central surface pressure is a more well defined quantity and more readily measured.

In can be measured either by a barometer on a met station, if one happens to be located near the centre, or it can be measured from an aircraft either by dropping a sonde into the eye or by measuring the pressure in the aircraft and make a simple correction based on the measured height. Already in the fifties it became clear that the central, minimum pressure P_c is well correlated with $V_{\max}$, whereas the size (e.g. eyewall radius) seems not to be correlated with $V_{\max}$ at all. In other words, there is no rule saying that larger cyclones necessarily have stronger winds. The central pressure therefore plays a dominant role in TC modeling as an intensity measure, even if the maximum sustained wind is a more direct measure of the threat to life and property.

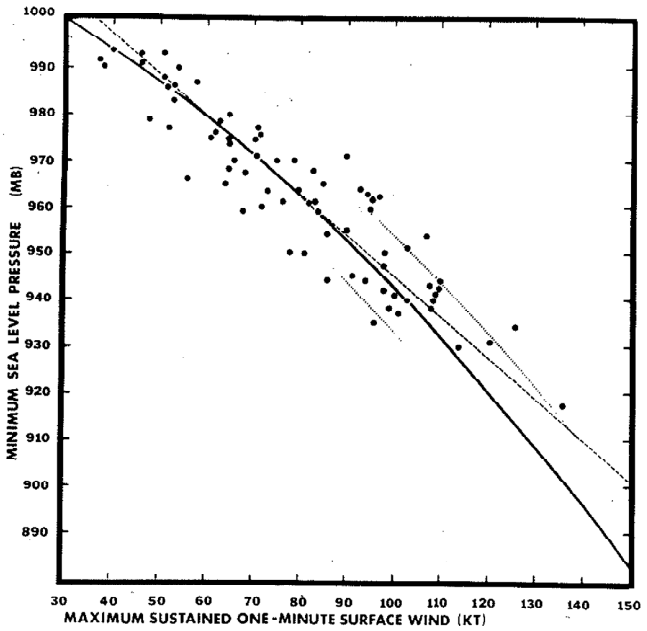

Figure 3. The $V_{\max} - P_c$ correlation of Atkinson and Holliday.

Atkinson and Holliday (1977) (hereafter referred to as A&H) established a correlation for P_c and V_{max} based on carefully selected data from surface stations that had suffered a 'direct hit' by a typhoon and where both pressure and wind speed had been recorded. In SI units the correlation can be written as

$$V_{\max} = V_{AH}\,(1 - P_c/P_n)^m \tag{1}$$

where V_{AH}=297 m/s, P_n=1010 hPa and m=0.644. Figure 3 shows the original plot with data points. Note that the straight line fits data just as well as (1). The relation is still in use and is in fact implicit in the Dvorak method so it is instructive to review the original paper.

The velocity records in those days were made with an ink pen on paper strips. It can be difficult to judge one minute or even ten minute averages from such a strip, hence A&H decided to read the maximum during a storm passage instead since this was easier. The paper gives an example of the further data processing. It is from the Andersen base in Guam where a met station was placed on a 191m high hill. The cup anemometer was placed 4m above the ground. This gives a total elevation of 195m above sea level which was then corrected for using a power law recommended by Sherlock in 1953. In other words, the hill was treated simply as an extension of the 4m mast. No attempt was made to account for speed–up effects of the hill nor for the actual 4m elevation of the anemometer. Next step was to convert the maximum value to a 1 minute average. A

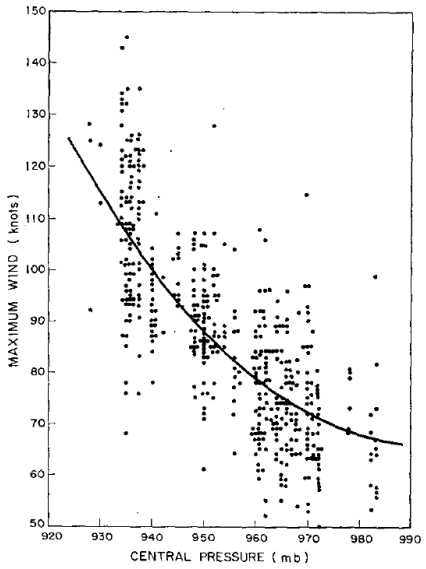

Figure 4. The $V_{\max} - P_c$ scatter plot based on reconnaissance flight data. $V_{\max}$ is probably measured at 900mb.

graph made by the the air force showing gust factor as a function of 1 minute wind speed was used for this. One problem with this is that the graph shows gust factors defined for an observation period of 1 minute while the paper strip record was several hours long. Another problem is that the gust factors in the graph were based on measurements over water while the station was on shore. Still worse, however, is the fact that the gust factor used for the correction decreases with wind speed (from 1.3 at 10m/s to 1.07 at 80m/s). Other observations of gust factors over water show no variation of the gust factor with wind speed. Vickery and Skerlj (2005) examined gust factor observations from hurricanes and found good agreement with the ESDU standard which suggests a slight *increase* with wind speed. Kristensen, Casanova, Courtney and Troen (1991) comes to the same conclusion for gust factors over water. The spuriously small gust factors used by Atkinson and Holliday imply an overestimation of the sustained wind. Such critique was raised by Black (1993) who suggested that a proper interpretation of the recorded gusts would produce a relation resembling one published by Fujita[1] in 1971. Fujita's relation is of the same form as (1) with the following values of the parameters: V_c=203m/s, P_n=1010hPa and m=0.569[2].

Harper (2002) gives a detailed discussion of these and various other issues with the A&H relation and comes to the following conclusion: 'Whilst the very substantive nature of the A&H work is acknowledged, it is possible that some of the surface wind speed es-

[1]Unfortunately we have not been able to retrieve the original paper.

[2]The parameters were derived from Harper (2002) who in turn got them from Black (1993)

timates at elevated sites are in error (inflated) due to topographic influences and that there is an increasing overestimation of surface winds for increasing wind speed (decreasing central pressure)'.

Harper also discusses the feasibility of a fixed pressure velocity relation as such. Figure 4, which has been reproduced from Shea and Gray (1973), shows measurements of $V_{\max}$ measured at the aircraft height (probably at the 900mb level) against the central pressure at sea level. Although the data are clearly correlated they are not confined to a very narrow band. Estimating $V_{\max}$ from P_c with fixed $P_c - V_{\max}$ relation will therefore only yield a very rough estimate.

A&H end their paper with the following remark: 'Hopefully, this wind-pressure relationship can be refined and improved in future years as more cases are added to this sample and more accurate techniques for measuring surface winds in tropical cyclones are developed.' Unfortunately, this did not happen. Even today, after another 30 years of tropical cyclone research, the Dvorak method still uses the original relation (we return to the Dvorak method below).

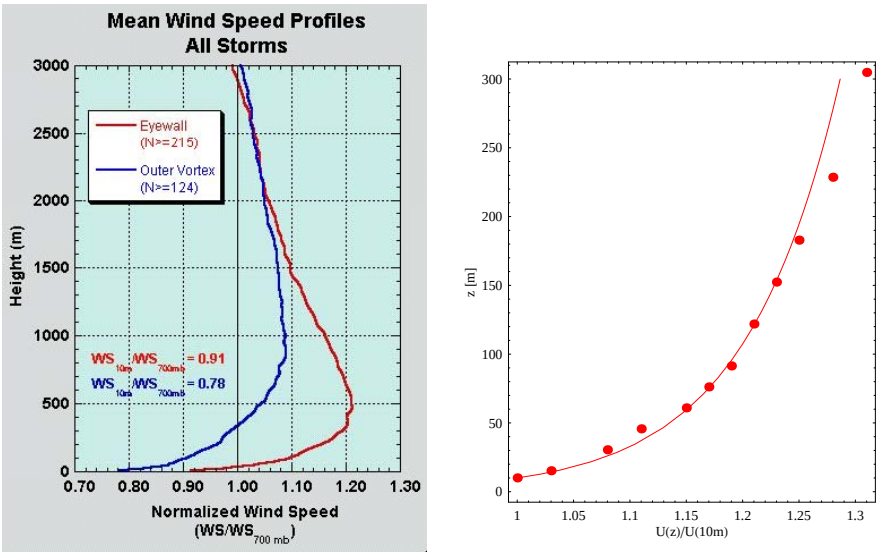

Figure 5. Left: Hurricane wind profiles obtained by GPS drop sondes. The wind speed at 700mb is used as reference since this is what is usually measured from aircraft. Right: Eyewall data plotted together with a logarithmic profile with $z_0 = 0.07mm$.

Recently the National Hurricane Center in Miami has investigated hurricane winds over the sea by GPS drop sondes, see Franklin, Black and Valde (2000). Figure 5, taken from the NHC home page, was obtained by averaging a large number of measurements. The eyewall profile has a maximum at about 500m. Plotting the data (available on the homepage) with a logarithmic z–axis shows that below 2-300m the profile is close to logarithmic with $z_0 \sim 0.1$mm. The logarithmic profile is characteristic of a horizontally homogeneous, neutrally stratified constant flux layer controlled by surface friction. Near the eyewall the air is unstable, and friction competes with both pressure and streamline curvature, each making contributions to the momentum budget about an order of magnitude larger than the friction (the Coriolis force contributes less). A several hundred meter deep constant vertical momentum flux layer therefore requires a rather delicate cyclostrophic balance, at least on average. It should be noted that profiles from individual drop sondes

are too irregular to show a deep logarithmic layer. Wind profile measurements over land were made by Amano, Fukushima, Ohkuma, Kawaguchi and Goto (1999) using acoustic sounding. The measurements show a logarithmic variation up to a maximum height Z_G above which the wind speed stays constant. Z_G, which is quite distinct, is typically on the order of 500m, but in some cases lower than 100m. The constant value $U(Z_G)$ in the top layer is consistent with the gradient wind for a Holland pressure profile with $B = 1$ (the model is explained in Section 3).

2.3 Comparison between JMA and JTWC best track data for 2000–2003

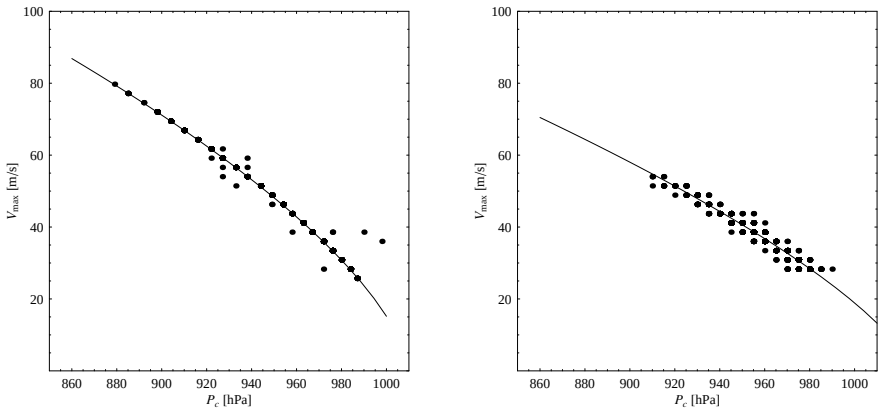

Figure 6. $V_{\max}$ vs. P_c for best track data (2001–2003). Left: JTWC estimates (points) and Atkinson–Holliday correlation (line). Right: JMA estimates (points) and a fitted regression line.

In the notes accompanying the JTWC best track data it is stated that 'comparisons of JTWC best-tracks with those of other agencies must be done with extreme caution'. The following warning is also found: 'Recent JTWC best-tracks also contain intensity estimates, although confidence in the quality of these estimates is low'. Nonetheless, this has not prevented us from comparing JMA and JTWC best track data – be it with or without 'extreme caution'.

Figure 6 shows $V_{\max}$ vs P_c for the two datasets for the years 2001–2003. The JWTC data points closely follow the Atkinson-Holliday correlation which is also shown. Actually the plot is a bit misleading since the rounding off makes many of the data points fall exactly onto each other. In reality the points that deviate from the correlation represent less than 2% of the data points. Conversely, the remaining more than 98 % of data points must have been estimated solely from the Dvorak method.

The $V_{\max}$ vs P_c plot for the JMA data is also shown in figure 6. The points also fall in a narrow band, though not as closely on a single curve as the JTWC data. The JMA methods have not been published, hence it is not possible to judge whether the scatter is due to input from other observations than satellite images. On JMA's homepage it is said that satellite images are used to deduce upper-air wind speeds by direct tracking of cloud

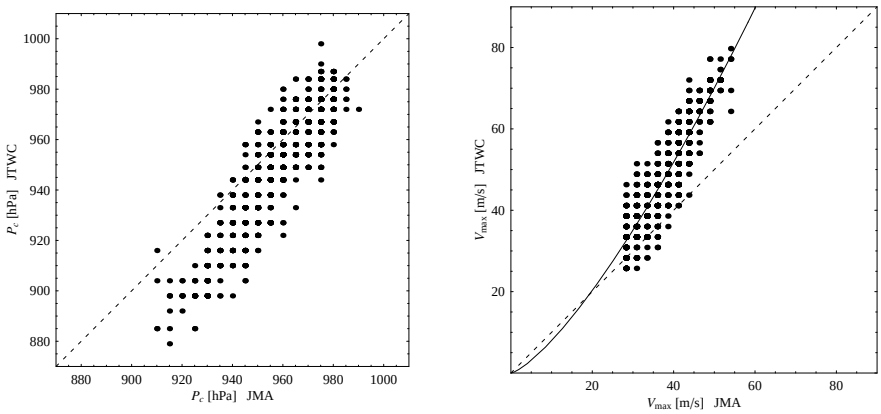

Figure 7. Comparison of estimated intensities from the JMA and JTWC best tracks data (2001–2003). Left: Central pressure. Right: Maximum sustained wind speed with regression line.

movements, and this might explain the deviations from a single curve. Image velocimetry is not part of the Dvorak method, but it is possibly part of JMA's methodology. JMA obviously use a different P_c–$V_{\max}$ relation, which happens to resemble the one obtained by Fujita in 1971 for Atlantic hurricanes.

JTWC defines wind speeds as one minute averages whereas JMA use ten minute averages as recommended by WMO. According to the JTWC home page this means that the maximum sustained winds given by JTWC should be about 14% higher than those given by JMA. However, when the best tracks are compared the difference is considerably larger. Figure 7 shows scatter plots comparing estimated maximum sustained winds and central pressures from JMA and JTWC for the years 2001–2003. The data were selected so that both time stamps and positions were in agreement, and it is most likely that the same satellite images were used by both JMA and JTWC for the analysis. Apparently with different results. The discrepancy is largest for the most intense storms, where it amounts to more than 40% in terms of $V_{\max}$. JMA generally estimates higher central pressures and combining this with a pressure–velocity correlation that yields lower velocities we end up with large differences.

It is difficult to draw conclusions about the two data sets because of lacking documentation and validation of the estimation methods. One rare example is shown in figure 8 reproduced from Martin and Gray (1993). Here the central pressure forecasts of NW Pacific typhoons made by JTWC during 1977–1986 using the Dvorak method is compared with aircraft data. A tendency for the satellite forecasts to underestimate P_c (overestimate the intensity) at the high intensity end of the scale is very clear, and the discrepancy seems to match the discrepancy between JTWC and JMA best track data. It should be noted that the comparison is for pressures which are forecasts. These could be more conservative than best track pressures which are hindcasts. Still, the figure indicates that a correction of the JTWC correlation between Dvorak intensity number and P_c is in order. JTWC did not do this, but perhaps the JMA did.

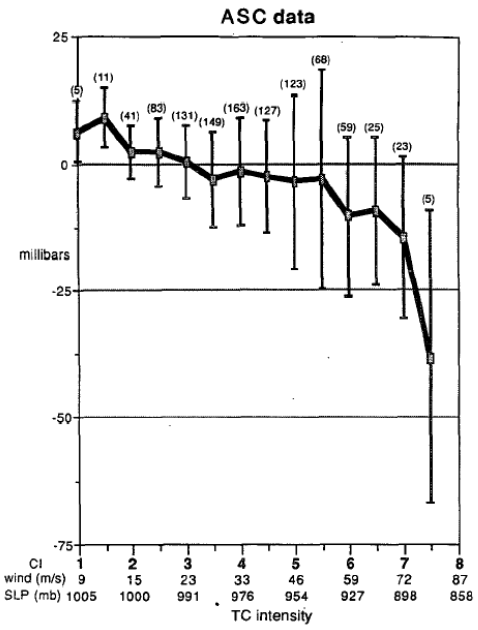

Figure 8. Comparison of intensity forecasts made by the Dvorak technique with aircraft reconnaissance data. The difference between satellite and aircraft central pressure is shown with 10% and 90% percentiles.

3 The Holland model

Holland (1980) (see also Harper and Holland 1999) proposed a simple tropical cyclone model, which we will use to interpret the best track data. Holland's model is generally recognized as a satisfactory model of the simple, engineering type. The model is based on the gradient wind V_g which is defined so that the radial component of the acceleration, $-V_g^2/r$ balances the pressure gradient and the Coriolis force:

$$V_g^2 = \frac{r}{\rho}\frac{\partial P}{\partial r} - frV_g \tag{2}$$

where f is the Coriolis parameter and ρ taken to be constant (=1.15 kg/m^3). Solving for V_g we get

$$V_g = -\frac{fr}{2} + \sqrt{\left(\frac{fr}{2}\right)^2 + \frac{r}{\rho}\frac{\partial P}{\partial r}} \tag{3}$$

Investigations by Willoughby (1990) show that gradient balance indeed exists at the flight levels of reconnaissance aircraft. When the surface pressure gradient is inserted into (3), V_g corresponds to a wind that would have been in the absence of friction. In figure 5 this corresponds to neglecting the lower 500m and extrapolate the upper part to the surface. Reading from the plot we find $V_g/WS_{700\mathrm{mB}} \sim 1.28$ at the eyewall and $V_g/WS_{700\mathrm{mB}} \sim 1.12$ at the outer edge. The ratio K_m between surface wind V_{rmmax} and the gradient wind turns out to be the same in both cases viz.

$$K_m \equiv V_{\max}/V_g \sim 0.9/1.28 \text{ or } 0.78/1.12 \sim 0.70 \tag{4}$$

in rough agreement with Harper (2002) who suggests $K_m = 0.75$. This value applies to a water surface.

Holland proceeds by prescribing $P(r)$ as

$$P(r) = P_c + (P_n - P_c)\exp\left(-(R_0/r)^B\right) \tag{5}$$

where P_c is the central pressure, P_n is the ambient pressure defined e.g. as the pressure corresponding to the last closed isobar, R_0 is a characteristic length and B is a dimensionless shape parameter. Holland found good agreement with data using this parametrization.

For small r the pressure gradient dominates over the Coriolis force and (2) reduces to

$$V_g \approx V_c = \sqrt{\frac{r}{\rho}\frac{\partial P}{\partial r}} = \sqrt{\frac{P_n - P_c}{\rho}B(R_0/r)^B}\exp\left(-(R_0/r)^B/2\right) \tag{6}$$

v_c, known as 'the cyclostrophic wind', has a maximum for $r = R_0$ so that we can identify R_0 as the eyewall radius R_w (R_w is typically just a few percent smaller than R_0 when $f \neq 0$ is taken into account). The maximum velocity at ten meter is given by

$$V_{\max} = K_m\sqrt{\frac{B(P_n - P_c)}{\rho \mathrm{e}}} \tag{7}$$

If we adopt the A&H relation (1) together with (7) then we end up postulating that

$$B = \frac{V_{\mathrm{AH}}^2 \rho \mathrm{e}}{K_m^2 P_n}(1 - P_c/P_n)^{2m-1} \tag{8}$$

Since $2m > 1$ this means that more intense (in terms of P_c) storms should be more peaked (have larger Bs).

The JMA track data list R_{50}, the radius to 50 knots wind speed, the central pressure P_c and the maximum sustained wind $V_{\max}$. The ambient pressure P_n is unknown, but it is conventional to adopt the value $P_n = 1010$ hPa. Following Holland we use $\rho = 1.15\,\mathrm{kg/m^3}$ and 0.7 is a plausible value for K_m as mentioned above. This is sufficient to determine the model parameters B and R_0.

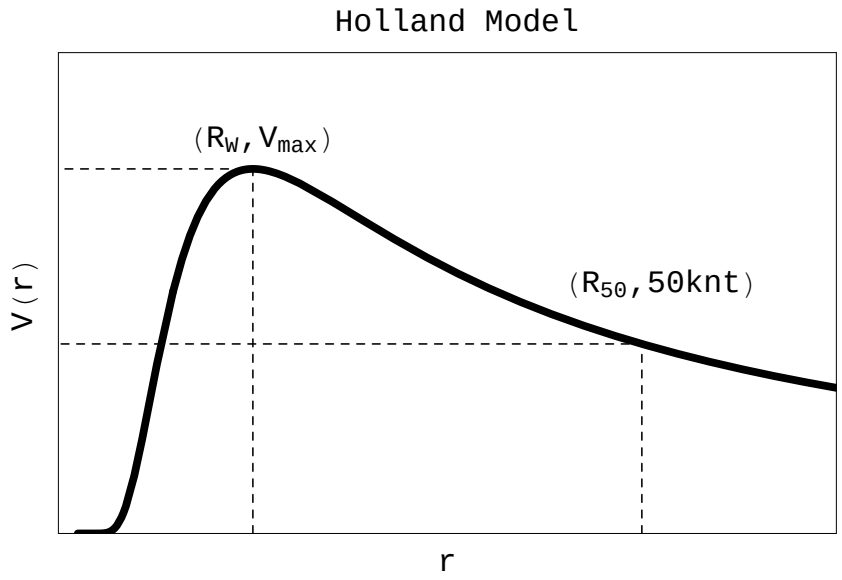

Figure 9. Schematics of the Holland velocity profile.

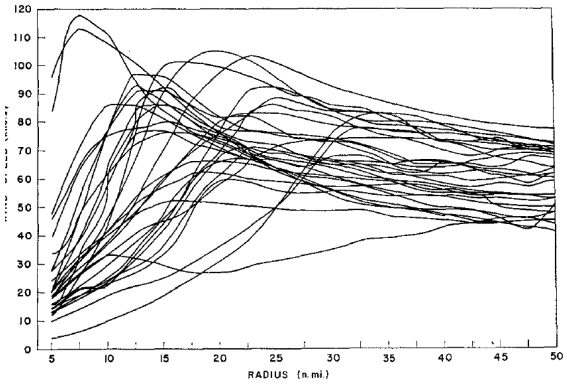

Figure 10. Sample of tangential wind profiles (from Shea & Gray 1973).

Holland demonstrated that his model yields fair results for wind profiles measured by aircraft flying at 700 hPa. It should be noted that Holland's validation is only for the central parts of the cyclone, out to about 3-4 times R_w. A more comprehensive validation of Holland's model was made recently by Willoughby and Rahn (2004) who compared it with aircraft measurements of almost 500 hurricane cases. The flights were made along constant pressure ($P = 700$ or 850mb) trajectories and the geopotential height $z(P)$ was recorded along with the wind speed at that height. In each case the hurricane was traversed several times with a number of crossings of the eyewall at different angles and at least covering centre distances between $R_w/2$ and $2R_w$. The data were processed in order to obtain the circular average of the tangential wind speed in a frame of reference following the storm centre. Some systematic flaws of Holland's wind profile were discovered. The width of the calm plateau around the centre is too broad in the model. The data show a more gradual, approximately linear, variation of the wind speed with r for $r \ll R_w$. At the inner side of the eyewall the model profile is too steep and the peak around the maximum velocity is broader than observed. Finally, the profile rolls off too fast beyond 2–3 R_w,

a feature that was also noted by Harper (2002). In the extreme value analysis we will choose to skip all velocities below 50 knots. For the JMA data R_{50}/R_w is seldom larger than 3 so the outer parts of the profile are not important for the present study. The model's behavior for $r < R_w$ is likewise unimportant, at least as far as maximum wind speeds are concerned, because points inside the eye sooner or later get hit by the maximum wind speed at the eyewall. The fact that the peak seems to be too broad in the model profile is more of a problem since it will tend to overestimate the area exposed to large wind speeds. Moreover, the tendency for a more pointed peak than prescribed by the model is most prominent for the more intense storms.

Although the validation of the Holland model leaves room for improvements of the prescribed pressure profile, it does, however, not discredit it substantially. Holland's velocity profile actually performs quite well. Fitted profiles reproduce data to within a mean bias of less than 1m/s, which is completely satisfactory compared to the conceivable uncertainties of wind speed estimates associated with the Dvorak method. RMS values for fitted profiles are about 4.5m/s on average. At the same time the model fitted the pressure data with a bias of 1 hPa and RMS value of 2 hPa. The 4.5m/s wind speed RMS is less satisfactory, but not alarming, and should probably be taken as a sign that no prescribed pressure profile would ever be perfect. In worst cases RMS deviations of individual profiles exceed 12m/s. These are hurricanes undergoing eyewall replacement cycles, which, in any case, cannot be expected to be adequately described by a simple model.

The measured winds used for the model comparison were averages over several flights to obtain an approximate averages over a circles. Therefore we should interpret the model profile as representative of the circular symmetric part of the flow without the inclusion of fluctuations. In other words, the model does not include the effects of meso-vortices and tornados.

4 Wind turbine loads during an eye-wall passage

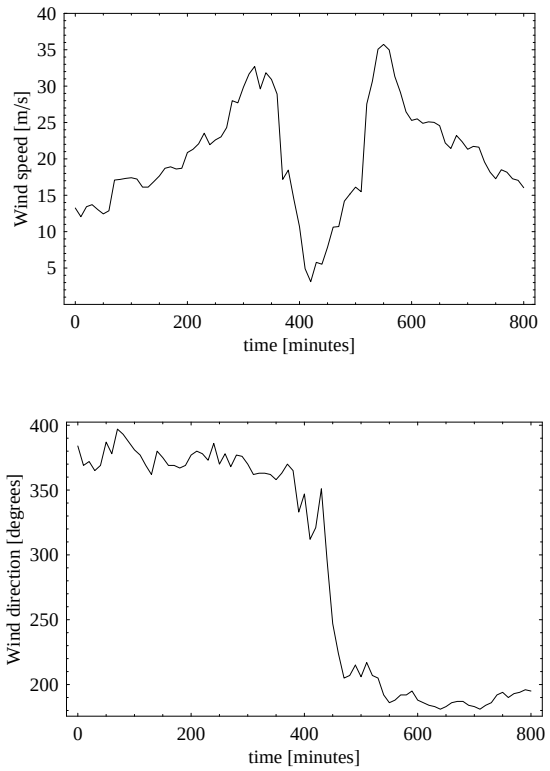

Figure 11. Ten minutes average wind speed and direction time series from a met station that encountered a direct hit by a TC.

Wind loads on wind turbines depends on how it is operated by the control system. Basically this is done by controlling yaw, the orientation of the rotor plane with respect to the wind direction, and pitch, the orientation of the blades. On older, stall regulated, types the pitch cannot be adjusted, but these are probably not suited for TC climates. Yawing is slow with a typical maximum yaw speed of about 1/2 degree per second. The pitch, on the other hand, can be adjusted almost instantly. At wind speeds lower than a certain cut–in wind speed the turbine stands still without yawing and pitching. At wind speeds moderately larger than the cut–in speed the pitch is controlled in such a way as to maximize power production. At still higher wind speeds (above about 10 m/s) the power production reaches its maximum dictated by the capacity of the generator and the pitch is regulated so as to maintain power production at a constant level. Above a cut–out wind speed (e.g. 25 m/s) the turbine is shut down in order to protect it. This can be done by stopping the rotation of the blades with brakes and minimizing thrust by adjusting the pitch so that the wind attacks the blade edges. Another strategy is to idle, i.e. to let the rotor run but pitch in such a way that no power is produced. At the same time yawing must continue so as to keep the rotor plane perpendicular to the wind direction. This is important in order to prevent fatal loads from occurring. It should be noted that the velocity at the tip of a rotating blade is around 60 m/s for most designs, which means that the blades are exposed to typhoon wind speeds whenever the turbine is producing. It

therefore seems less likely that a blade would be the first part of the construction to yield.

The strongest winds in a TC are found at a radius which almost coincides with the radius of the eyewall. Figure 11 shows measured wind speeds and directions from a met station that encountered a direct hit by a TC. Two wind speed maxima are seen corresponding to the two passages of the eyewall while the wind direction changes counterclockwise by 180°. For a wind turbine the second passage of the eyewall is critical if both wind speed and direction changes rapidly. Because of the low wind speed in the eye it is likely that the control system shuts down. As the eye passes the wind direction changes 180°, but the turbine may not yaw because the wind speed is low. If so and if the wind returns rapidly at the second passage of the eyewall, the turbine could be forced to yaw 180° in a short time. Assuming a maximum yaw speed of 1/2 degree per second this operation takes 6 minutes. To this comes a delay because the control needs a certain time to detect a change of wind direction (if it were to respond to all fluctuation of the wind direction the yaw mechanism would quickly be worn down). A critical situation can obviously arise if the yaw is not in place before the wind returns. For the passage depicted in figure 11 the wind turns rather slowly (less than 0.1 deg./s) and should not cause problems for a wind turbine. Figure 10 (reproduced from Shea and Gray (1973)) gives an impression of the large variability of $V(r)$ profiles. The time it takes for the wind to return at the second passage depends on the slope of the $V(r)$ curve as well as the advection speed V_a (the velocity of centre).

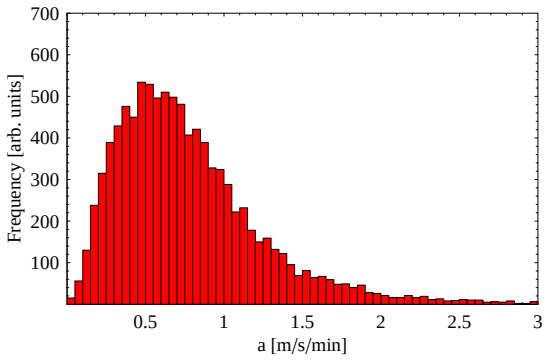

Figure 12. Histogram showing frequencies of a (see text for definition).

We can use the maximum value of the 'acceleration'

$$a = \frac{dV(r)}{dt} = V_a \frac{dV(r)}{dr} \tag{9}$$

as a measure of how fast the wind returns. Using the Holland model with parameters obtained from best track data (from JMA) we get the histogram depicted in figure 12. From this it appears that the wind speed very rarely changes by more than 10m/s in ten minutes, a value which should not pose any problems for a wind turbine. However, this estimate of a is based on an idealized, circular symmetric, mean wind profile which in reality is strongly perturbed. On top of the mean wind field there will be local thunderstorms and so–called spin–up vortices. A spin–up vortex is a vortex which is being stretched along its axis of rotation. The stretching has the effect of increasing the rotation speed much in the same way as when an ice dancer makes a pirouette. The conditions near the eyewall seem to favor vortex stretching and in severe cases this can lead to the formation of regular tornados. Tornados are small relative to the general TC circulation, only a few hundred meters, but very intense. Tornados are not confined to the eyewall, but may occur several hundred kilometers away from the centre. Meso–vortices are a few kilome-

ters wide, thus larger than tornados but smaller than the TC. They occasionally form in the eyewall. Hurricane-spawned tornados were studied by Novlan and Gray (1974) who listed all known tornados that occurred in hurricanes in US in the period from 1948 to 1972. In this period tornados were observed in about 25% of all tropical storms making landfall in the US. According to Novlan and Gray 'tornados contribute up to 10% of the fatalities and up to half a percent of the damage caused by hurricanes that spawn them'. Most tornados occur over land within 200 kilometer from the shore and they mostly form where the wind blows onto the shore. Novlan & Gray attribute tornado formation to the large low–level vertical wind shear that occurs while a TC makes landfall. These conclusions are in line with a similar Japanese study by Fujita, Watanabe, Tsuchiya and Shinada (1972) and later studies.

5 Extreme winds

In this section we will set up a statistical theory for tropical typhoons. The idea is to use Holland's model to calculate the winds surrounding the centre out to the 50 knot radius R_{50}. By definition the maximum sustained wind speed should be at least 50 knot for a tropical cyclone to be regarded as a typhoon (and get a name), so it is natural to choose this limit to define the width of the typhoon. Another good reason for making such a cut off is that the Holland model is known to predict too large wind speeds far away from the eye. In the analysis we will therefore simply neglect wind speeds below 50 knot.

The wind speeds we will work with are ten minutes averages sampled at 10m. Shorter averaging times, which could also be relevant, can be derived from ten minutes averages assuming universal statistical relations.

Theoretically extreme winds could occur outside tropical cyclones, for example in isolated thunderstorms. In this analysis we assume that the contributions from other mechanisms than typhoons are negligible. In a more detailed analysis the neglected wind field outside the typhoon could perhaps be accounted for e.g. by reanalysis data. Even better would it be to analyse long and reliable records from met stations. The passage of a typhoon can be determined from the best track and the passage can be identified on the wind speed time series, thus enabling separate statistical analysis of extreme winds caused by typhoons/hurricanes and by other mechanisms. This was done for North Australian extreme winds by Cook, Harris and Whiting (2003) who used three classes of mechanisms: hurricanes, thunderstorms and 'other mechanisms'. They found that although thunderstorms in some places contribute to many of the annual maxima, the fifty year recurrence wind speed (defined below) was still determined by the contribution from hurricanes so that the two other mechanisms could be neglected. We assume that this is also the case in the western North Pacific.

Various definitions of 'the fifty year wind speed', U_{50}, can be found in the literature. Kristensen et al. (1991) suggest to define a gust as a wind speed that on average is exceeded once during the recurrence period T. Such a definition implicitly assumes that exceedances are isolated, independent events, like clicks from a Geiger counter, that can be described by a Poisson process. We therefore briefly recall properties of such a process before returning to the definition of U_{50}.

For a Poisson process the probability of having n events during the reference period t is equal to

$$F(t,n) = \frac{(\lambda t)^n}{n!}\,\mathrm{e}^{-\lambda t} \tag{10}$$

where λ is the *event rate*. In particular, the probability of not observing any events during t is

$$F(t,0) = \mathrm{e}^{-\lambda t} \tag{11}$$

The expected number of events during a period of length t is equal to

$$\langle n\rangle = \sum_{n=0}^{\infty} nF(t,n) = \lambda t \tag{12}$$

Taking the recurrence period is the reference period for which $\langle n\rangle = 1$, simply yields $t = 1/\lambda$. Alternatively we can define the recurrence period so that the probability that no event occurs is equal to e^{-1}. From (11) we get the same result: $t = 1/\lambda$. We will use the latter definition here since it is the most general. The reason for this is that periods with no events are easy to identify. Otherwise, if events occur, then we will have to find out exactly how many. For clicks from a Geiger counter this is simple, but for wind speeds it not obvious exactly what an 'event' really is. We cannot simply say that each time the wind speed exceeds a certain threshold we have an event, because such events are not independent since they will typically occur in cascades caused by storms. It is slightly better to use 'up–crossing' events, defined each time the wind speed crosses from below

to above the threshold. This eliminates multiple counting of consecutive exceedances. However, typhoons usually give two wind speed peaks, one for each of the two passages of the eyewall, which are obviously not two independent events. Alternatively we can place a 'dead time' window around each exceedance in which other exceedances should not be counted. The window would typically be a few hours wide corresponding to the time it takes for a storm to pass. However, according to an investigation of Scottish data by Brabson and Palikof (2000) a three–hour dead time window does not make events completely independent. In fact their data show a positive correlation over time scales as long as 160 hours indicating that storms may not occur as independent events. Seasonal variations is another complication. In Scotland almost all major storms occur during winter, and typhoons also have a season. Proper event counting is therefore not trivial because an underlying Poisson process can be hard to identify.

However, we can make things work without postulating an underlying Poisson process. First, we assume that exceedances which are sufficiently separated in time are independent. More specifically, we will assume that a separation of 1 year is sufficient for this independence. Second, we assume that wind speeds for different years have identical statistical properties. This ensures stationarity of wind speed time series. It should be noted that the validity of this assumption is debatable; conflicting views can be found in Pielke, C. Landsea and Pasch (2005) and (. Webster, Holland, Carry and Chang 2005) For the present analysis the assumed stationarity implies a neglect of any effect of climate changes.

Now, let $F_1(x)$ denote the cumulative distribution function (cdf) of the wind speed u taken over a reference period of one year. Thus $F_1(x)$ is the probability that u stays below the threshold value x for a full one year period, or the probability of not observing any exceedances of the threshold x in one year. We will write $F_1(x)$ as

$$F_1(x) = \mathrm{e}^{-\Lambda_1(x)} \tag{13}$$

where $\Lambda_1(x)$ can be interpreted as the mean number of events per year for a Poisson *ghost process* that happens to reproduce the observed $F_1(x)$. We can always define Λ in this way even if the ghost process does not have physical reality. Due to the assumed independence between different years, the cdf for a T year period, $F_T(x)$, is given by

$$F_T(x) = \big(F_1(x)\big)^T = \mathrm{e}^{-\Lambda_1(x)T} \tag{14}$$

Thus $F_T(x)$ complies with the same ghost process as $F_1(x)$. It is therefore natural to define the recurrence period $T(x)$ in terms of recurrence period of the ghost process:

$$T(x) = 1/\Lambda_1(x) = -T/\log F_1(x) \tag{15}$$

With this definition we have circumvented the event counting problem. There is no need for a procedure that finds the effective number of independent exceedances since we are in effect concentrating on periods with no events. Thus $T(x)$ can be characterized as the mean *waiting time* to the next exceedance of the threshold x starting from a point in time where there has been no recent exceedances (within a year or so). This definition makes good sense when dealing with mechanical structures. Here the threshold represents a critical wind load beyond which the construction is damaged (or where there is no guarantee that it will not be damaged). Once an exceedance occurs the damage is done, and it really does not matter if the exceedance is followed by a cascade of exceedances. We are therefore mostly interested in the safe periods, and $T(x)$ is the mean duration such periods.

5.1 The Gumbel distribution

If we assume that the event rate has an exponential form:

$$\Lambda(x) = \exp\left\{-\frac{x-\beta}{\alpha}\right\} \tag{16}$$

where α and β are two parameters, then the cumulative distribution becomes a Gumbel distribution

$$F(x) = P(u < x) = \exp\left[-\exp\left\{-\frac{x-\beta}{\alpha}\right\}\right] \tag{17}$$

The variable u should denote the annual maximum of the wind speed so that $F(x)$ is equal to the probability that the wind speed u stays below the threshold value x during one year. Assuming that annual maxima are independent, this means that the probability of not exceeding x during T years is equal to $F^T(x)$. The T-year maximum, u_T therefore has the distribution

$$F(x;T) = P(u_T < x) = [P(u < x)]^T = \exp\left[-T\exp\left(-\frac{x-\beta}{\alpha}\right)\right] = \exp\left[-\exp\left(-\frac{x-\beta-\alpha\log T}{\alpha}\right)\right] \tag{18}$$

which is also a Gumbel distribution just with β replaced by $\beta + \alpha\log T$. The fact that $F(x;T)$ takes the same functional form for all T is very convenient. Conversely, we can ask which distributions have this property, i.e. satisfy the relation

$$f^T(x) = f\left[\frac{x-b(T)}{a(T)}\right] \tag{19}$$

where f is a 'universal' function of a single variable and $a(T)$ and $b(T)$ are functions of T. The problem was solved by Fisher & Tippet (see Gumbel 1958). The solution can be cast in the general form

$$\begin{aligned} a(T) &= a(1)T^{-T} \\ b(T) &= b(1) - ca(1)(T^{-c} - 1) \\ f(s) &= \exp\left[-(1+cs)^{-1/c}\right] \text{ for } 1+cs > 0 \end{aligned} \tag{20}$$

where c is a shape parameter. The restriction $1+cs > 0$ places a lower bound on s when $c < 0$ and an upper bound when $c > 0$. In the limiting case $c \to 0$ we get the Gumbel distribution. It should be noted that there is no magic with extreme value distributions that says that they should always apply to extreme values. If x follows an extreme value distribution then the same will not generally hold for a function of x, say $g(x)$. Conversely, we can always find a function g so that $g(x)$ follows an extreme value distribution. So it is only if we can argue for (19) from knowledge of the physical system under consideration that we can hope to prove that F is an extreme value distribution. On the other hand, in dealing with extreme values we are not often blessed with very many data points and it is quite impossible to *reject* an extreme value distribution for x (or for x^2). Experience with annual maxima of the wind speed shows that the Gumbel distribution seems to fit data for practical purposes, hence we choose a Gumbel distribution.

It is tempting to use the generalized extreme value distribution since this allows one more fitting parameter. However, when the number of data points is small there is a risk of 'overfitting' the data. This is illustrated in Brabson and Palikof (2000) where generalized extreme value distributions were applied to a 13 year subset of a 39 year long data record. Comparing the 100 year wind predicted from the 13 year subset with that based the whole record they found poorer results when using a generalized extreme value distribution than when using a Gumbel distribution.

5.2 Estimation of U_{50}

In this section we discuss three methods to determine the Gumbel parameters α and β from a set of n independent observations $\{u_1, u_2, \ldots u_n\}$. All methods use order statistics i.e. the observations are ordered and renamed to $\{x_1, x_2, \ldots x_n\}$ where $\{x_1 < x_2 < \ldots < x_n\}$.

In Gumbel's (1958) method a cumulative probability F_j is assigned to each x_j. Gumbel notes that

$$\langle F(x_j)\rangle = \frac{j}{n+1} \tag{21}$$

where $\langle * \rangle$ denotes the mean value, and therefore chooses $F_j = \frac{j}{n+1}$. Then $-\log(-\log(F_j))$ is plotted against x_j and a straight line is fitted to the points either by eye or by a least square fit with equal weights. The line is expected to be $y = (x-\beta)/\alpha$ which determines the parameters. This is the traditional method. It is sometimes stated that it yields a central estimate of U_{50}, but this is not true. The problem is that $-\log(-\log(\langle F(x_j)\rangle)) \neq \langle -\log(-\log(F(x_j)))\rangle$, so the fitted line is shifted in a systematic way. In practical cases this leads to over–predictions of U_{50} by a few percent.

Harris (1996) proposed to use the exact value $\langle -\log(-\log(F(x_j)))\rangle$ in the plot and weight the least square fit with the inverse variance of $-\log(-\log(F(x_j)))$. This produces a more central estimate of U_{50}.

A somewhat different approach was followed by Abild, Mortensen and Landberg (1992). His method is based on the following two statistics

$$B_1 = \frac{1}{n}\sum_{j=j}^{n} x_j \tag{22}$$

$$B_2 = \frac{2}{n(n-1)}\sum_{j=1}^{n}(j-1)x_j \tag{23}$$

For a Gumbel distribution it can be shown that

$$\begin{aligned} \langle B_1\rangle &= \beta + \alpha\gamma \\ \langle B_2\rangle &= \beta + \alpha\gamma + \alpha\log 2 \end{aligned} \tag{24}$$

where $\gamma = 0.577\ldots$ is the Euler constant. The parameters are obtained by equating B_1 and B_2 with their mean values and solving (24). This yields

$$\begin{aligned} \alpha &= \frac{B_2 - B_1}{\log 2} \\ \beta &= B_1 - \alpha\gamma = \frac{\gamma+\log 2}{\log 2}B_1 - \frac{\gamma}{\log 2}B_2 \\ U_{50} &= \beta + \alpha\log 50 = \frac{\gamma-\log 25}{\log 2}B_1 - \frac{\gamma+\log 50}{\log 2}B_2 \end{aligned} \tag{25}$$

Note that B_1 is just the average of all observed values (ordered or not). B_2 can be characterized as the mean value of biannual maxima. Biannual maxima can be generated by randomly selecting two annual maxima and discard the lowest. The j-th value x_j is chosen if it is picked together with x_1 or $x_2\ldots$ or x_{j-1}, hence the weight $j-1$. With this interpretation in mind it is clear that B_1 and B_2 are central (bias free) estimates of $\langle B_1\rangle$ and $\langle B_2\rangle$, and hence the estimate of U_{50} is also central because it is a linear combination of B_1 and B_2. We will use this characterization to make two generalizations of the method.

First we consider censored data, i.e. data where observations below a cut–off u_0 have been deleted. The typhoon data are of this type since they only represent wind speeds above 50 knot. This means that annual maxima can be missing since there is a chance that u_0 is not exceeded during a particular year. We will choose to make up for missing annual maxima simply by filling the cut–off value u_0 into the vacant places. With k missing values we thus have $x_j = u_0$ for $j \leq k$. This changes the cdf to

$$F_{\text{cens}}(x) = \begin{cases} F_1(x) & \text{for } x > u_0 \\ \\ 0 & \text{for } x < u_0 \end{cases} \tag{26}$$

where F_1 is the Gumbel cdf (17). We can still use B_1 and B_2 as estimates of $\langle B_1 \rangle$ and $\langle B_1 \rangle$, but because of the changed cdf (24) is replaced by

$$\langle B_1 \rangle = u_0 + \alpha(\log \Lambda + \gamma + \Gamma(0, \Lambda)) \tag{27}$$

$$\langle B_2 \rangle = u_0 + \alpha(\log 2\Lambda + \gamma + \Gamma(0, 2\Lambda)) \tag{28}$$

where $\Gamma(t,k)$ is the incomplete gamma-function and Λ is defined in terms of α, β and u_0 by the relation

$$\beta = u_0 + \alpha \log \Lambda \tag{29}$$

Defining the function

$$g(\Lambda) = \log \Lambda + \gamma + \Gamma(0, \Lambda) \tag{30}$$

it follows that

$$\frac{\langle B_2 \rangle - u_0}{\langle B_1 \rangle - u_0} = \frac{g(2\Lambda)}{g(\Lambda)} \tag{31}$$

Inserting the estimates B_1 and B_2 into the left hand site this equation can be used to determine Λ and subsequently α, β and U_{50} can be determined by the relations

$$\alpha = \frac{\langle B_1 \rangle - u_0}{\log \Lambda + \gamma + \Gamma(0, \Lambda)} \tag{32}$$

$$\beta = u_0 + \alpha \log \Lambda \tag{33}$$

$$U_{50} = \beta + \alpha \log 50 = u_0 + \alpha \log 50\Lambda \tag{34}$$

This completes the first generalization.

The second generalization is the following. Suppose that we have a number of observation points located so closely together that it can be assumed that they all share the same Gumbel distribution. For example, the observation points could be nearby met stations or they could be points on a grid where annual maxima have been obtained from best typhoon tracks. We assume that annual maxima from different years are independent and equally distributed, also when they belong to different observation points. However, annual maxima for different stations are allowed to be correlated when they are from the **same** year. With these assumptions we can get a better estimate of $\langle B_1 \rangle$ by averaging the B_1 values for each of the observation points. Possible correlations does not affect the average so it is still a central estimate. In the same way B_2, averaged over the observation points, yields a central estimate of the mean biannual maximum. U_{50} can therefore be obtained as described above using the improved estimates of $\langle B_1 \rangle$ and $\langle B_2 \rangle$.

5.3 Comparison of U_{50} estimates

A numerical exercise was conducted in order to check the methods of Gumbel (1958), Harris (1996) and Abild et al. (1992). Sets $\{u_1, u_2 \ldots u_n\}$ of independent numbers were generated by letting

$$u = -\log(-\log(F)) \tag{35}$$

where F is a random number equally distributed on $[0,1]$. This produces independent samples from a Gumbel distribution with $\alpha = 1$ and $\beta = 0$. The three methods were then used to estimate U_{50} and these were compared with the exact value $U_{50} = \log 50$.

Table 1 shows the results in terms of bias and rms error for Gumbel distributed datasets generated in this way. Two values of n were used: $n = 10$ and $n = 28$. The numbers in the table are based on 100000 sets (for each n) and should be significant to two digits. Gumbel's method makes the poorest performance due to larger bias than the other two. The positive bias signifies over–prediction. Harris' method evidently corrects this, but not entirely, while Abild's method is a true central estimate. For $n = 10$, relevant for ten years of data, Abild's method performs best, closely followed by Harris's method.

For $n = 28$, relevant for the present study, Abild's method is only marginally better than Harris's method.

Table 2 is similar to Table 1 except that the data were censored. All values below $u_0 = -\log(-\log(0.25))$ were discarded corresponding to a 25 % chance of not getting a annual maximum. We note that Abild's method no longer yields a central estimate of U_{50}. This is due to the fact that U_{50} is a non–linear function of $\langle B_1 \rangle$ and $\langle B_2 \rangle$ for censored data. However, the ranking of the methods is unchanged.

This numerical exercise indicates a slightly better performance of Abild's over the other two methods and hence Abild's method is used in the following.

Table 1. Performance of the three methods for Gumbel distributed data.

	Gumbel	Harris	Abild
Mean bias, $n = 10$	1.02	0.39	0.00
Mean bias, $n = 28$	0.54	0.17	0.00
Rms error, $n = 10$	1.97	1.36	1.26
Rms error, $n = 28$	1.08	0.75	0.74

Table 2. Performance of the three methods for censored Gumbel distributed data. The cut–off u_0 has been chosen so as to yield 25 % missing data.

	Gumbel	Harris	Abild
Mean bias, $n = 10$	1.00	0.36	0.24
Mean bias, $n = 28$	0.56	0.16	0.07
Rms error, $n = 10$	2.18	1.67	1.67
Rms error, $n = 28$	1.21	0.89	0.87

6 Extreme wind atlas for the NW Pacific

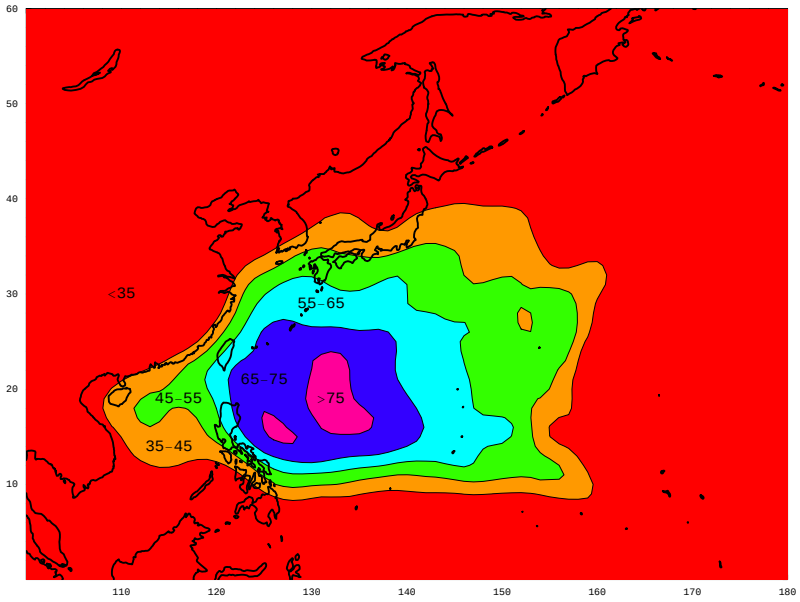

Figure 13. U_{50} (in m/s) based on JMA best tracks for the western North Pacific

A square one–by–one degree grid of 'observation points' covering the western North Pacific region (0N–60N and 100E–180E) was used for the extreme wind analysis. The Holland model was used to estimate wind speed profiles for the JMA best tracks. Only parts of the tracks with a maximum sustained wind exceeding 50 knots were used and the profiles were cut off at 50 knots as well. In other words, all wind speeds below 50 knots were discarded. The Holland model parameters B and R_0 were fitted using $p_n = 1010$hPa and with values of p_c, $V_{\max}$ and R_{50} (radius to 50 knots wind speed) taken from the best track database. The data cover the period 1977–2004 where these data are available. For each typhoon track the grid points within the 50 knot zone around the eye was found and the corresponding maximum velocities were calculated. Sets of 28 annual maxima were then obtained for each grid point. The variant of Abild's method for censored data described above was then used to estimate grid point values of U_{50}. B_1 and B_2 were first calculated for each grid point and these values were then averaged over 3 by 3 neighboring grid points to estimate $\langle B_1 \rangle$ and $\langle B_2 \rangle$ and subsequently U_{50} as described above.

Figure 13 shows a contour plot of the resulting extreme wind estimates for the western North Pacific. The 'typhoon ally' NE of the Philippines is prominent and the weakening caused by landfall on the continent and larger islands (Japan) is also evident.

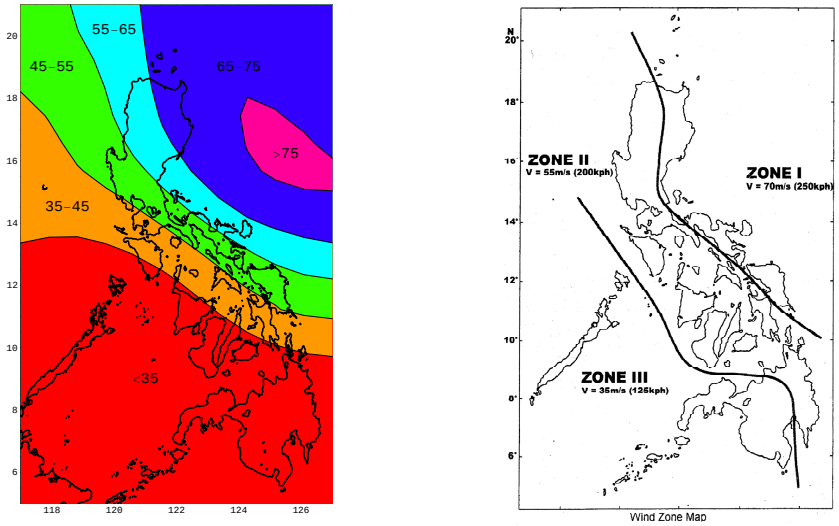

Figure 14. Extreme winds in the Philippines. Left: U_{50} from analysis of JMA best tracks. Right: 50 year gust zones according to the Philippine National Structural Code for Wind Loads.

Figure 14 shows results for the Philippines together with a figure taken from the Philippine Building Code. This figure shows three zones with different 'characteristic wind' V. According to the code V is defined as the fifty year 3 second gust measured 10m over flat terrain with a roughness of 3cm. The ten minute average wind speeds from the JMA data correspond, we believe, to a measurement taken 10m meter *above sea level*. Therefore V and U_{50} are not directly comparable, but the shapes of the U_{50} contours roughly follow the V–zone divisions.

7 Validation

Due to the uncertainties associated both with the best track data and with their interpretation in terms of the Holland model it is important to make checks against surface measurements. By courtesy of the Climate Data Section at the Philippine Atmospherical, Geophysical and Astronomical Services Administration (PAGASA), we have obtained a set of historical observations of extreme wind data from Philippine met stations.

Rellin, Jesuitas, Sulapat and Valeroso (2001) summarize extreme wind observations made at Philippine met stations operated by the Philippine Atmospheric, Geophysical and Astronomical Services Administration (PAGASA) in the period 1948–1996. The data include a maximum windspeed observed in a given month during the whole period. Taking the maximum over all twelve months yields the maximum observed wind speed for the whole 49 year period for the station in question. The data show large geographical variations of the extreme wind. The general trend is that the extreme wind are stronger in the northern part of the country than in the southern part and stronger on eastern shores than on western shores. This is agreement with the general typhoon pattern with east–to–west running tracks. For two stations data is available in the form of data reports containing tables of observed extreme wind speeds during tropical cyclone passages for the period 1948–2003. The two stations are: Basco (Pagasa 2005a) located on the Batan Island and Aparri (Pagasa 2005b) located at the northern shore of Luzon.

According to PAGASA the observations are read by eye from pointer instruments by an observer, but the precise procedure is not known to us. The numbers given in the reports are simply referred to as 'observed extreme wind speeds' without further discussion. Therefore we do not know how often the observations are made and for how long the pointer instrument is observed or if the reading is an estimated average or a peak value or at which height the anemometer is placed (probably 10m). The station data have time stamps which do not seem to form a regular pattern. It is possible that readings are normally taken at regular intervals, but that during a TC passage readings are made more or less continuously. Data is missing for about 25% of the passages, perhaps due to evacuation of the personnel. Table 3 shows that discrepancies exist between the sources. Although these data are far from perfect, 49 years of observations from 46 stations is still an impressive record.

Table 3. Maximum observed wind speeds (in km/h) for 1948–1996 according to different sources. A:Rellin et al. (2001), B:Pagasa (2005a) and B:Pagasa (2005b)

Station	Source	Jan	Feb	Mar	Apr	May	Jun	Jul	Aug	Sep	Oct	Nov	Dec
Basco	A	130	90	108	94	158	166	224	212	216	155	94	–
Basco	B	–	–	–	176	158	166	223	212	216	241	194	47
Aparri	A	94	108	90	122	79	198	180	151	180	209	191	90
Aparri	C	–	–	–	122	79	112	108	101	144	270	151	54

7.1 Data from the Province of Batanes

Batanes, the smallest province in the Philippines in terms of population and land area, is composed of ten islands and islets located about 270 north of the mainland Luzon and 160 km from the southermost point of Taiwan. The inhabitants, called Ivatans, have a unique culture and speak their own language. The region is passed by a typhoon once every three years on average, and, having no means of escaping, the Ivatans are used to stay put in their well build stone houses and 'ride out the gale'. The Ivatans have a reputation of being 'tough guys' among Filipinos.

The data set (Pagasa 2005a) consists of various statistics for typhoons that encountered the Batanes Province during the period 1948–2003. Of special interest is a table of

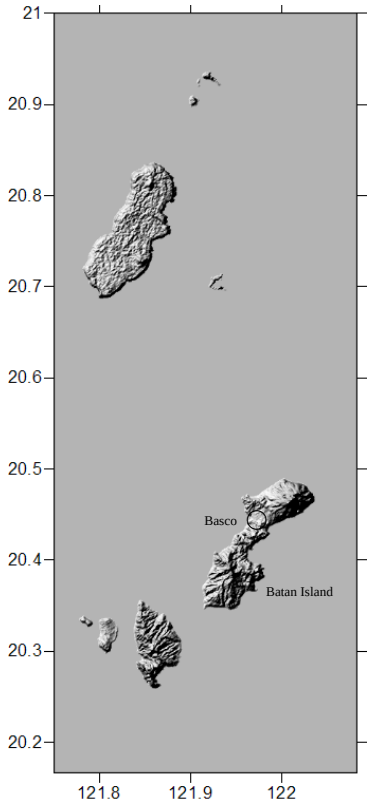

Figure 15. The islands comprising the Batanes Province. The circle marks Basco on Batan Island

observations made at the Basco Synoptic Station located on the Batan Island. The island is a 16 km long and 2–4 km wide with a 1000m high mountain at the NE end and a 400m high mountain at the SW end. A more shallow two km wide strip of land connects the two mountains. The observation position, given as 20°30′00”N 121°50′00”S, is located close to the airport NE of Basco town and SE of the northern mountain.

The data report lists all tropical cyclones that passed within a radius of 200 km of the station. The table contains observed maximum wind speed and direction during each passage (a blank entry indicates missing data) as well as the amount of rainfall, but no pressure data.

The observed wind speeds were read from an analog pointer instrument. The procedure consists in observing the pointer for a few minutes and then note the maximum value and an estimated average value. The tabulated values are probably the maxima. Although this procedure is normally repeated only at regular intervals, it appears from the irregular time stamps that the instrument was probably read more often during TC passages in order not to miss the maximum value during the passage. We believe that the anemometer is of the Pitot tube type with a response time of a few seconds. This would correspond to a measurement of the 3 second gust defined in the Philippine National Structural Code for Wind Load.

The records appear to be accurately kept, especially for the three latest decades that overlap the best track data. There are relatively few entries with missing data in this period. This allows us to extract annual maxima with some confidence.

Figure 16 shows a Gumbel plot ($-\log(-\log F(u))$ vs. u) of the annual maxima for Basco met station. The plot shows a good fit to a straight line thus confirming the Gumbel distribution. The data cover the years 1976–2003. The lowest annual maximum, only 4m/s in 1989, seems spuriously low and is probably a misprint, so this year was discarded.

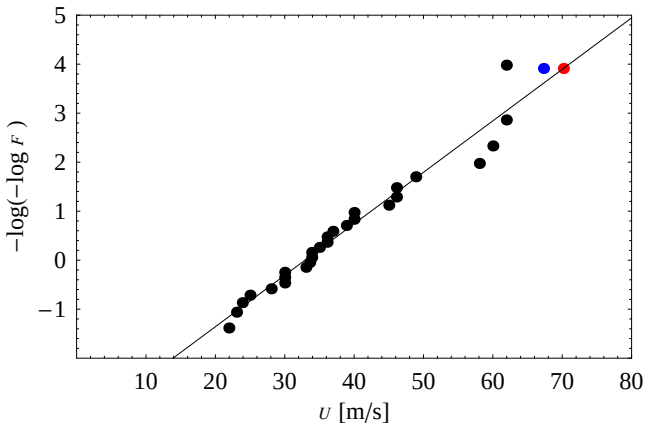

Figure 16. Black dots: Gumbel plot of observed annual maxima at the Basco met station. Line: $y = (x - \beta)/\alpha$. Red dot: U_{50} calculated from data. Blue dot: U_{50} from best track analysis.

The estimates of the Gumbel parameters, based on the remaining 27 years of annual maxima, are

$$\alpha = 9.5\text{m/s}, \qquad \beta = 32.9\text{m/s}, \qquad U_{50} = 70.2\text{m/s} \tag{36}$$

This should be compared with the estimates from the best track analysis which yields

$$\alpha = 7.3\text{m/s}, \qquad \beta = 32.2\text{m/s}, \qquad U_{50} = 67.3\text{m/s} \tag{37}$$

Judged from Monte Carlo simulations the statistical errors on the estimates of U_{50} are about 10m/s, so the agreement is excellent. However, it might also be fortuitous because the exact conditions are not known, and this goes for the observed data as well as the best track data. The best track wind speed probably refers to a water surface even for tracks over land. In order to correct to a rougher surface the model results should be reduced by 10–20%. The observed wind speeds should be corrected for averaging time which might lead to a similar reduction. Local orography can also influence the readings.

7.2 Comparison with Philippine Extreme wind data

Extreme winds observed at Philippine met stations have been reported by Rellin et al. (2001). As discussed above uncertainty exists as regard the observation procedure, averaging times and measurement heights and descriptions of the local orography are lacking (thus preventing estimation of the surface roughness). In order to compare the model with observations, the observations should ideally be corrected for orography effects (i.e. speed–up on hill tops) and effect of local surface roughness and averaging time, but this has not been done. Figure 17 shows the observed 49–year maxima U_{max49} on a map of the Philippines. From this it is clear that the NE parts are more exposed than the SW parts and that typhoons are generally rare in the south. The standard deviation of the observed maxima is about 10 m/s. The scatter between values for nearby stations seem larger which might be explained by local influence of terrain.

At 43 out of a total of 49 stations the observed U_{max49} exceeds 25m/s, signalizing that they were hit by one or more typhoons. The model predicts non–zero probability of typhoon hits on 40 stations. In 38 cases model and observations are in agreement that the station is endangered by typhoons and in 4 cases they agree on no typhoons. In the remaining 6 cases there is disagreement: 2 cases where the model predicts typhoons which were actually not observed and 4 cases where it is visa versa. When no, or very

few, tracks pass over a station the model prediction is not meaningful, so in order to make a fair comparison we have plotted the 38 cases where both model and observations agree on non–zero typhoon frequency, see figure 18. 9 of the remaining 11 stations, which are not shown on the figure, are located south of the 9th latitude. For the last two there is considerable disagreement. At Baler met station located on Luzon Island in the north the recorded $U_{\text{max49}} = 25\text{m/s}$ is very low compared to neighboring stations. At the Puerto Princesa met station (the most westerly station) $U_{\text{max49}} = 49\text{m/s}$ is recorded whereas no best tracks passed the area in 1977–2003. The high value might be caused by a single typhoon passing the area prior to 1977.

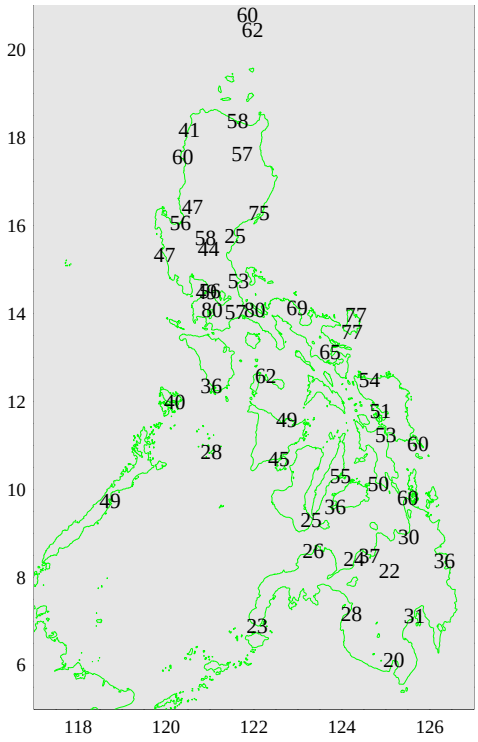

Figure 17. Maximum wind speed for the whole period 1948–1996 observed at Philippine synoptic station.

For a Gumbel distribution the mean value of the 49 year maximum is equal to

$$\langle U_{\text{max49}} \rangle = \beta + \alpha \log 49 + \alpha\gamma = U_{49} + \alpha\gamma \tag{38}$$

$\langle U_{\text{max49}} \rangle$ is therefore somewhat larger than U_{49}. The standard deviation of the difference between model results and observations is 10m/s. With a statistical uncertainty of about 5–10m/s for both model and observation this amount of scatter is to be expected. Fitting the data to the relation $y = ax$ yields $a = 0.96$, surprisingly close to 1. However, the observations are more spread out than the model predictions and there is a tendency for the model to under–predict large values and over–predict small values. This could be a due to the pressure–velocity correlation used by JMA in connection with the Dvorak method, but there could be other reasons such as local terrain effects.

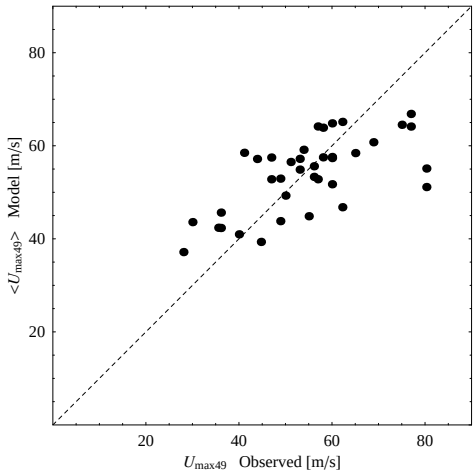

Figure 18. Comparison of model predictions of the mean value of the 49 year maximum wind vs. observed maxima for Philippine met stations that have experienced typhoon wind speeds ($> 25 m/s$) during 1948–1996.

8 Conclusions

A model for extreme winds in the western North Pacific based on best track data from JMA has been developed. Holland's model was used to generate wind speed profiles from the best track data from which sets of annual maxima could be made for specific locations. Assuming a clipped Gumbel distribution and using a modification of Abild's method, the fifty year wind was then determined.

The best track data were reviewed. Unfortunately the methods by which the best track are derived are poorly documented. It seems that the Dvorak method is the main, and perhaps the only, method which is applied. Therefore this method was discussed. From this it appears that the empirical basis for the estimates is weak, in particular for the maximum sustained wind speed. The method relies on a pressure–velocity correlation on which there does not seem to be consensus and which in reality is a rough approximation. A comparison between beat track data from JMA and JTWC shows huge differences in estimated wind speeds. The JMA data were selected mainly because they provide maximum wind speed data for a sufficiently long period (28 years) to enable reliable estimates of extreme winds to be made. A validation in terms of a direct comparison of the surface wind speeds predicted by the Dvorak method and ground observations does not seem to exist. This is a major disadvantage.

Holland's model which is used to 'hang' velocity profiles on the tracks implies some simplifications. The model predicts a circular symmetric wind field which in most cases is an excellent approximation to the large scale features of the actual wind field surrounding a tropical cyclone. This means a neglect of small scale structures in the flow. These are sometimes found in the form of meso–vortices, spinning sub–systems a few kilometers wide orbiting the centre, or even tornados. Wind turbines are particularly vulnerable to small, vortices because they induce rapid wind direction changes. Little is known about the statistics of meso–vortices and tornados in typhoon, but the indication is that they are after all too rare to influence the fifty year wind.

Three different methods to fit a Gumbel distribution to data were tested. Of these Abild's method was found to be the best. A generalization of the method which treats data from a number of nearby stations was made and employed to make an extreme wind atlas for 50 year winds in the western North Pacific.

Comparison of model results with data from synoptic stations in the Philippines shows good agreement within the expected statistical scatter, although with a tendency for under–prediction of large wind speeds and under–prediction of low wind speeds. However, there are many uncertainties with the observed data and corrections for surface roughness, orography and averaging time could not be made, hence the agreement could be fortuitous.

References

Abild, J., Mortensen, N. G. and Landberg, L.: 1992, Application of the wind atlas method to extreme wind data, *J. Wind Eng. Ind. Aerodyn.* **41–44**, 473–484.

Amano, T., Fukushima, H., Ohkuma, T., Kawaguchi, A. and Goto, S.: 1999, The observation of typhoon winds in Okinawa by Doppler sodar, *J. Wind. Eng. Ind. Aerodyn.* **83**, 11–20.

Atkinson, G. and Holliday, C.: 1977, Tropical cyclone minimum sea level pressure/maximum sustained wind relationship for the western North Pacific, *Mon. Wea. Rev.* **105**, 421–427.

Black, P.: 1993, Evolution of maximum wind estimates in typhoons, *Proc. ICSU/WMO Int. Sym. on Tropical Cyclone Disasters, Beijing, China*, International Council of Scientific Unions, pp. 104–115.

Brabson, B. B. and Palikof, J. P.: 2000, Tests of generalized Pareto distributions for predicting extreme wind speeds, *Journal of Applied Meterrology* **39**, 1627–1640.

Cook, N. J., Harris, R. I. and Whiting, R.: 2003, Extreme wind speeds in mixed climate revisited, *Journ. of Wind Eng. and Indust. Aerodyn.* **91**, 403–422.

Dvorak, V.: 1975, Tropical cyclone intensity analysis and forecasting from satellite imagery., *Mon. Wea. Rev* **103**, 420–430.

Franklin, J., Black, M. and Valde, K.: 2000, Eyewall wind profiles in hurricanes determined by GPS dropwindsondes, *Proc. 24th Conf. Hurricanes and Tropical Meteorology*, AMS, pp. 448–449. URL http://www.nhc.noaa.gov/aboutwindprofile.html.

Fujita, T. T., Watanabe, K., Tsuchiya, K. and Shinada, M.: 1972, Typhoon-associated tornados in Japan and new evidence of suction vortices in a tornado near Tokyo, *J. Meteor. Soc. Japan* **50**, 431–453.

Gumbel, E. J.: 1958, *Statistics of Extremes*, Columbia University Press.

Harper, B. A.: 2002, Wind-pressure relations and related issues for engineering planning and design, *Technical Report J0106-PR003E*, Systems Engineering Australia Pty Ltd. URL http://www.uq.net.au/seng/download/Wind-Pressure%20Discussion%20Paper%20Rev%20E.pdf.

Harper, B. and Holland, G. J.: 1999, An updated parametric model of the tropical cyclone, *Proc. 23rd Conf. Hurricanes and Trop. Meteo.,10–15 Jan, Dallas,Texas*, AMS, pp. 104–115.

Harris, R. I.: 1996, Gumbel revisited — a newlook at extreme value statistics applied to wind speeds, *Journ. of Wind Eng. and Indust. Aerodyn.* **59**, 1–22.

Holland, G.: 1980, An analytic model of the wind and pressure profiles in hurricanes, *Mon. Wea. Rev.* **108**, 1212–1218.

Kristensen, L., Casanova, M., Courtney, M. and Troen, I.: 1991, In search of a gust definition, *Boundary-Layer Meteorol.* **55**, 91–107.

Martin, J. and Gray, W.: 1993, Tropical cyclone observation and forecasting with and without aircraft reconnaissance, *Weather and Forecasting* **8**, 519–532.

Novlan, D. J. and Gray, W. M.: 1974, Hurricane–spawn tornados, *Mon. Wea. Rev.* **102**, 476–488.

Pagasa: 2005a, Information on tropical cyclones province of Batanes (1948–2003), *Technical report*, Data report from Climate Data Section, Climatology and Agrimeteorology Branch, Pagasa.

Pagasa: 2005b, Information on tropical cyclones province of Cagayan (1948–2003), *Technical report*, Data report from Climate Data Section, Climatology and Agrimeteorology Branch, Pagasa.

Pielke, Jr., R. A., C. Landsea, M. Mayfield, J. L. and Pasch, R.: 2005, Hurricanes and global warming, *Bulletin of the American Meteorological Society* **86**, 1571–1575.

Rellin, M. F., Jesuitas, A. T., Sulapat, L. R. and Valeroso, I. I.: 2001, Extreme wind hazard mapping in the Philippines, *Technical report*, N0. 111, The Philippine Atmospheric, Geophysical and Astronomical Services Administration (PAGASA).

Shea, D. J. and Gray, W. M.: 1973, The hurricane's core region. i. symmetric and asymmetric structure., *Journal of the Atmospheric Sciences* **30**, 1544–1564.

Vickery, P. J. and Skerlj, P. F.: 2005, Hurricane gust factors revisited, *Journal of Structural Engineering* **131**, 825–832.

Webster, P. J., Holland, G. J., Carry, J. A. and Chang, H.-R.: 2005, Changes of tropical cyclone number, duration and intensity in a warming invironment, *Science* **309**, 1844–1846.

Willoughby, H. E.: 1990, Gradient balance in tropical cyclones, *Journal of the Atmospheric Sciences* **47**, 265–274.

Willoughby, H. E. and Rahn, M. E.: 2004, Parametric representation of the primary hurricane vortex. Part I: Observations and evaluation of the Holland (1980) model., *Monthly Weather Review* **132**, 3033–3048.

Risø's research is aimed at solving concrete problems in the society.

Research targets are set through continuous dialogue with business, the political system and researchers.

The effects of our research are sustainable energy supply and new technology for the health sector.